1

Crustal conditions favoring convective downward migration of fractures in deep hydrothermal systems

Sæunn Halldórsdóttir[1], Inga Berre[1], Eirik Keilegavlen[1], and Gudni Axelsson[2]

[1]University of Bergen, Center for Modeling of Subsurface Dynamics, Department of Mathematics, University of Bergen, Allégaten 41, 5007 Bergen.

[2]ÍSOR, Icelandic GeoSurvey, Urdarhvarf 8, 203 Kópavogur.

Corresponding author: Sæunn Halldorsdottir (saeunn.halldorsdottir@uib.no)

Key Points:

- Numerical modeling supports convective downward migration of fractures as a source mechanism for hydrothermal systems

- Fluid flow, fracture opening and propagation in a thermo-poroelastic rock mass are simulated in different geological settings in the crust

- Crustal stresses are key to understanding whether a hydrothermal system can evolve in regions away from active zones of volcanism

Abstract

Cooling magma plutons and intrusions are the heat sources for hydrothermal systems in volcanic settings. To explain system longevity and observed heat transfer at rates higher than those explained by pure conduction, the concept of fluid convection in fractures that deepen because of thermal rock contraction has been proposed as a heat-source mechanism. While recent numerical studies have supported this half a century old hypothesis, understanding of the various regimes where convective downward migration of fractures can be an effective mechanism for heat transfer is lacking. Using a numerical model for fluid flow and fracture propagation in thermo-poroelastic media, we investigate scenarios for which convective downward migration of fractures may occur. Our results support convective downward migration of fractures as a possible mechanism for development of hydrothermal systems, both for settings within active zones of volcanism and spreading and, under favorable conditions, in older crust away from such zones.

Plain Language Summary

Geothermal energy is transferred through and stored in the rock and fluids of the earth's crust. If temperature increases sufficiently with depth and the crust provides sufficient pathways for water to flow through, colder water sinks and percolates downward, gets heated at depth and then rises due to its lower density at higher temperature. This creates a hydrothermal circulation system that transports heat from the deep crust to shallower depths from where it can be produced. Wells drilled into these systems produce hot water and/or steam for direct heat utilization or electricity production. To understand the renewability of hydrothermal systems, we need to understand how heat is transferred deep in the crust. A hypothesis has been proposed, suggesting that fractures, propagating downwards because of contraction of the water-cooled surrounding rock, are central to maintaining the heat transfer from the deep crust. Based on settings in Iceland, we show how the fluid flow and propagation of fractures can be important for development of hydrothermal systems, using computer simulations, both in active regions of volcanism and, under favorable conditions, also in older crust away from such regions. The latter results are important for the identification of hidden geothermal systems.

1 Introduction

Hydrothermal fluid circulation within the earth's crust is driven by the combination of sufficient heating from below and permeability for fluids to flow (Lapwood, 1948). It is an important mechanism of mass and heat transfer in the crust and is seen as the explanation of anomalous temperature profiles with depth that are not consistent with heat transfer by conduction alone (Elder, 1965; Pálmason, 1967). While the concept was originally developed considering porous rocks, it was later expanded to include rocks with secondary permeability in the form of fractures, dikes and other structural features providing the main fluid conduits (Bodvarsson & Lowell, 1972). For hydrothermal systems, Bodvarsson and Lowell (1972) suggested how contraction induced by buoyancy-driven convective cooling would lead to tensile fracture opening and consequently strongly affect permeability at depth. A conceptual model of fractures migrating downwards due to convective cooling was described further by Lister (1974) and Bodvarsson (1982), including also analytical estimates of propagation speeds based on simplifying assumptions. Bodvarsson (1982) was the first to name the process "convective downward migration of fractures" (CDM) and specifically considered its role in transferring heat from cooling magma bodies to hydrothermal system over the lifespan of the hydrothermal

61 activity. As the magma cools, a layer of gradually thickening solidified rock develops, providing
62 an insulation between the heat source and the hydrothermal system. If this layer is impermeable,
63 and the intrusive intensity of the magma is low, heat transfer from the magma to the
64 hydrothermal system will decrease with time, which is inconsistent with the high heat output of
65 such systems over long time scales (Bodvarsson, 1982; Björnsson et al., 1982). For hydrothermal
66 systems in Iceland, Bodvarsson (1982) argued that the intrusive intensity would be low, and,
67 hence, hypothesized CDM to be an important mechanism for heat transfer.

68 Bodvarsson, (1982; 1983) and Axelsson (1985) also suggested that CDM could be
69 effective as a source mechanism in systems with elevated heat flux but away from central
70 magmatic heat sources, and may account for some of the long-lasting low-enthalpy hydrothermal
71 activity in the Icelandic crust. For such settings, they both proposed that the onset of the process
72 would depend on local stress conditions. Such settings are not only limited to Iceland but can
73 also be found in other areas (Jolie et al., 2021; Limberger et al., 2018). A better understanding of
74 the settings controlling the highly coupled processes governing CDM may therefore also shed
75 light on the existence of hydrothermal systems in other parts of the world.

76 While a comprehensive understanding of the geological settings where CDM can occur is still
77 lacking, two recent numerical modeling studies support the hypothesis. Patterson & Driesner,
78 (2021) present a model of large-scale natural convection in a downward propagating fracture
79 zone (of dimensions: H=3km, L=8km, W=1m) in a thermo-elastic medium, considering what we
80 in the present context will denote a low geothermal gradient of 55°C/km. They investigate the
81 effect of thermoelastic rock stresses and fracture fluid pressure on fracture-zone transmissivity
82 by use of a Barton-Bandis relationship between fracture transmissivity and effective normal
83 stress (Bandis et al., 1983; Barton et al., 1985). Expanding on the conceptual model by Lister
84 (1974) and Axelsson (1985), Stefansson et al., (2021b) present a fully coupled numerical
85 approach for fracture propagation and deformation that allow for multiple fractures in a thermo-
86 poroelastic medium. The effect of thermo-poroelastic stresses on fracture transmissivity is
87 incorporated through a fracture contact mechanics model. In the work of Stefansson et al.
88 (2021b), the downward migration of fractures due to convective cooling is considered for a test
89 case with a set of smaller fractures (H=200m, L=200m, W=2mm) at the bottom of a geothermal
90 system. The study applied parameters which are representative for a geothermal system in a
91 geological setting with a high geothermal gradient of 150°C/km.

92 In this paper we use numerical modeling to investigate CDM as a source mechanism for
93 hydrothermal activity. We consider both young crust in active zones of volcanism and spreading
94 as well as older crust away from such zones. The numerical approach builds on the methodology
95 by Stefansson et al. (2021b), accounting for flow and fracture propagation in thermo-poroelastic
96 media. This enables us to study effects of the stress regime and thermal gradients, as well as
97 effects of important rock parameters such as the permeability in the medium surrounding the
98 fractures. The results by Stefansson et al. (2021b) indicate that CDM can be a plausible source
99 mechanism in systems away from central heat sources if the thermal gradient is sufficiently high.
100 Furthermore, it is clear that local stress setting (e.g. in spreading systems) can be favorable for
101 CDM. This leads to the following hypotheses:

102   1. No central magmatic heat sources are needed for CDM, a high geothermal gradient is
103   sufficient to maintain the process.

104   2. With lower geothermal gradients, crustal stress conditions in a range of geological
105   settings are still favorable for CDM as a mechanism for heat transfer.

106 Using simulation models, we test these hypotheses with different thermal gradients, and show
107 how, for lower thermal gradients found away from volcanic belts, local stress settings are a
108 dominating factor for the onset of CDM.

109 As basis for the simulations, geological conditions found in Iceland are chosen. Iceland is
110 famous for its hydrothermal systems providing its nation with both electricity and space heating
111 through the utilization of geothermal fluids. Zones of spreading and volcanism cut through the
112 center of the country along the Mid-Atlantic Ridge, explaining the elevated heat content in its
113 crust. The volcanic belts rockmainly consist of very long fracture-zones dominated by spreading
114 and injection of extremely long dikes at depth. Several central volcano complexes are
115 interspersed in the zone, but these take up a very small part of the total area of the zone. For the
116 study of CDM two regional settings are chosen, (1) within the spreading zone but away from any
117 central volcanoes and (2) away from the spreading zone. Those two settings provide scenarios
118 with elevated heat flux, that we in the present context will denote by a high geothermal gradient
119 on one hand and low geothermal gradient on the other hand. As discussed in section 2, similar
120 settings can be found in other regions of the world.

121 **2 Geological settings for CDM**

122   Compared to normal conditions on the earth's surface, the heat flux through
123 hydrothermally active areas is elevated. In systems located within volcanically active areas one
124 might assume that intense magma intrusion frequency and resulting conduction, could at least
125 partly sustain these systems (Björnsson et al., 1982; Gunnarsson et al., 2010); however, this is an
126 unlikely case for most systems (Bodvarsson, 1954; Hochstein, 1995; Weir, 2001). We will look
127 at the effect of thermal stress changes, induced by cooling at depth by buoyancy driven
128 convection, and how this process can lead to enhanced permeability and heat transfer by
129 convection in propagating fractures. The process of fracture propagation at depth allows for
130 thermal fluid being in direct contact with hot formation deep within the systems (White, 1968;
131 Björnsson et al., 1982; Bjornsson & Stefansson, 1987). The process evolves over time to give
132 fluid access to new parts of the rock, which can be related to the lifetime and the intensity of
133 hydrothermal activity. Hence, CDM should be considered as a possible source mechanism of
134 hydrothermal activity.

135 We study a model of vertical fractures in the roots of geothermal systems, first proposed by
136 Lister (1974) and Bodvarsson (1982). Convection of geothermal fluid in the fractures cools down
137 the surrounding rock, causing horizontal tensile stresses in the rock, which lead to (1) the rock to
138 contract and (2) the fractures to propagate downward. By this self-sustained process, the
139 convection of thermal fluid extends downward constantly reaching fresh hot rock, enhancing the
140 heat flux to the geothermal system above. The process, combined with heat conduction, could
141 sustain the hydrothermal systems in accordance with observed heat output.

142   2.1 Extension deformation that favors vertical permeability

143   Areas of elevated heat flow and heat content that favor the development of hydrothermal
144 systems are located at divergent plate boundaries, where the spreading of the lithosphere leads to
145 ascending magma and intrusion into the crust. Regional extension tectonics create both regional
146 and local structures that furthermore affect permeability. Some examples of divergent plate

147 boundaries include the Mid-Atlantic Ridge, Red Sea Rift, Baikal Rift Zone, East African Rift
148 (Great Rift Valley), East Pacific Rise, Gakkel Ridge, Galapagos Rise, Explorer Ridge, Juan de
149 Fuca Ridge, Pacific-Antarctic Ridge, and West Antarctic Rift System. Many hydrothermal
150 systems are located in those settings, for example in Iceland (mid-Atlantic Ridge), Eritrea,
151 Djibouti, Ethiopia, Uganda, Kenya, Tanzania and Malawi (western and eastern branches of the
152 East Africa Rift) (Hochstein, 2005). Hydrothermal vents along the seabed are known to form
153 along divergent mid-ocean ridges, such as the East Pacific Rise and the Mid-Atlantic Ridge
154 (Petersen et al., 2018).

155 Divergent plate boundaries are examples of extension-controlled tectonics. Extension
156 deformation that can enhance vertical permeability can also be found in locations away from
157 convergent or transform plate boundaries, such as in back-arc basins (Lau Basin in the East
158 Pacific), in continental extension zones (Rio Grande Rift Zone, East-African Rift Zone, Western
159 Turkey (Bozkurt & Mittwede, 2005), and in releasing bends along strike-slip faults and in zones
160 of thickened crust (gravitational spreading). Known areas of hydrothermal activity associated
161 with continental rifting are, for example, located in the Great Basin in Western USA, the
162 countries in the western and eastern branches of the East African Rift, in west Turkey and in
163 Cyprus (Bettison-Varga et al., 1992; Murat Özler, 2000). Areas of hydrothermal activity
164 associated with back-arc activity are e.g. located in the Taupo Volcanic Zone New Zealand
165 (Kissling & Weir, 2005), and the Okinawa Trough Japan (Halbach et al., 1989; Yang et al.,
166 2020).

167 Extension deformation due to reginal tectonics alone can act to enhance vertical permeability and
168 therefore give rise to the circulation of fluids at intermediate depths in the crust. This, however,
169 does not explain increased hydrothermal activity in tectonically less active areas. Pálmason,
170 (1981) speculated on the effect of cooling of the lithosphere as it moves away from the rift axis
171 and suggests that thermal stresses consequently induce enhanced vertical permeability for
172 geothermal fluids at depths on the flanks of the active rifting. Hence, we consider the effects of
173 fluid circulation in existing fractures and how increased thermal stress may cause fracture
174 propagation, thus increasing vertical permeability. It is expected that both temperature settings in
175 the crust and regional stresses influence the initiation and maintenance of CDM.

176 **3 Mathematical and numerical modeling of CDM**

177 We use a mathematical model based on a discrete fracture matrix representation. The
178 medium is 3D, consisting of the rock matrix and embedded fractures modelled as 2D planes. The
179 model describes energy transport and fluid flow in rock matrix and fractures, thermo-poroelastic
180 deformation of the rock, and fracture deformation and propagation. We assume single phase
181 fluid conditions with the reservoir rock fully saturated, and with local thermal equilibrium
182 between the fluid and the solid. We impose a balance of momentum, mass and energy in the rock
183 matrix and a balance of mass and energy in the fractures, along with kinematic constraints and
184 constitutive laws for fracture deformation (Stefansson et al., 2021a; see also Barton, 1976). In the
185 following, key components of the model are reviewed. A full description of the mathematical
186 model, including coupling between variables in the rock matrix and the fracture (Jaffré et al.,
187 2011; Martin et al., 2005; Stefansson et al., 2021b), is provided in the supplementary material of
188 this paper.

189 Dimension reduction of the balance equations which is necessary to derive the flow of mass and
190 energy in the fracture is detailed in Stefánsson et al. (2021a) and Keilegavlen et al. (2021a).

191 The aperture of a dimensionally reduced fracture is given by

$$a = a_0 + [\![\mathbf{u}]\!]_n. \tag{1}$$

192 Here, a_0 is the residual hydraulic aperture in the undeformed state, and $[\![\mathbf{u}]\!]_n$ the normal
193 component of a displacement-jump over the fracture, defined as the difference in the
194 displacement, $\mathbf{u}$, computed on the opposing fracture walls. The fracture aperture, a, will be
195 affected by fluid pressure as well as thermo-poromechanical forces in the matrix. The flow in the
196 fracture is described by Darcy's law with a cubic law for the permeability, giving a strongly non-
197 linear relation between the aperture and the fluid flow.

198 We consider propagation due to tensile forces, modeled by the stress intensity factor (Stefansson
199 et al., 2021b; se also Nejati et al., 2015),

$$SI_{\mathrm{I}} = \sqrt{\frac{2\pi}{R_d}} \left(\frac{\mu}{\kappa + 1} [\![\mathbf{u}]\!]_n \right), \tag{2}$$

200 where R_d is the distance between the point where the displacement jump is evaluated and the
201 fracture tip, μ is the shear modulus of the rock, and κ is the Kolosov constant for plain strain
202 described as a function of the shear and the bulk moduli of the rock (see supplementary
203 material). The fracture tip propagates when SI_{I} exceeds a critical value,

$$SI_{\mathrm{I}} \geq SI_{Icrit}, \tag{3}$$

204 which can be viewed as the rock toughness.

205 The mathematical model is implemented in the open-source simulation tool PorePy,
206 which is tailored for representing complex multiphysics processes in fractured porous media
207 (Keilegavlen et al., 2021a). The fractures are explicitly represented in the computational grid
208 which allows for direct modelling of processes in the fracture and on the fracture walls. In the
209 computational grid, pressure and temperature are represented in both rock matrix and fractures,
210 the displacement is confined to the rock matrix and on the fracture walls, and contact tractions
211 are represented on the fractures. Fracture propagation is represented by extending the fracture
212 grid, with minimal adjustments needed to the rest of the computational model.

4 Simulations of CDM in different geological settings

214 Two regional settings are considered to investigate the process of CDM as a source
215 mechanism for hydrothermal activity. They are both considered representative of temperature
216 conditions in the crust of Iceland: (1) within the Icelandic active zone of volcanism and
217 spreading and (2) in older crust away from the active zone of spreading. The first represents
218 regions rich with geothermal resources while the second represents regions which are considered
219 to include fewer geothermal systems (Axelsson, et al., 2005). The heat source is thermal energy
220 within the earth's crust, accumulated over time by heat flow from the lithosphere and intrusive
221 activity. The background thermal gradient is 100-150°C/km (Flóvenz & Saemundsson, 1993) in
222 young crust within the rifting zone, and varies between 50° and 100°C/km in older crust further
223 away from the divergent ridge axis. These settings are distinct from known volcano complexes
224 with associated high-enthalpy hydrothermal activity and heat sources of magmatic origin.

225 The depth at which fissures are assumed to be open varies between those regions: Close to the
226 divergent axis, within the active zone, we assume fissures to be open down to 2 km depth,
227 whereas away from the axis, in colder crust, we assume fissures to be open down to 1 km depth.
228 Isothermal temperature with depth profiles from geothermal fields in Iceland strengthen this

229 assumption (Arnórsson et al., 2008; Axelsson, et al., 2000; Björnsson et al., 2000; Xianghui,
230 2012). We assume that the depth of open fissures reflect the depth of the geothermal systems in
231 the initial state of the simulations. Since we are investigating the longevity of the systems and the
232 CDM as a key mechanism to maintain the systems, we consider the opening and propagation of
233 fractures beyond those depths.

234   4.1 Simulation domain and setup

235   For the numerical investigation of different geological settings, we choose a three-
236 dimensional domain, a cube with side-lengths of 400 m. At the top of the domain, five evenly
237 spaced vertical planar fractures are located along the x-axis, each spanning 200 m in length and
238 depth. The formation depth and thermal gradients are set in accordance with the two regional
239 settings: For the two regional settings considered, the geothermal gradient is set accordingly to
240 (1) 130 °C/km and (2) 80 °C/km, representing temperature conditions within and away from the
241 active zone, respectively. The top of the simulation domain is located at (1) a depth of 2000 m
242 and (2) a depth of 1000 m, respectively, thus the temperature at the top of the domain is 260 °C
243 and 80 °C, respectively, for the two different cases. We denote settings corresponding to (1) as
244 high-temperature (HT) regimes and settings corresponding to (2) as low-temperature (LT)
245 regimes, respectively.

246 The background stress field is aligned with respect to the fractures, with vertical stress (S_V) equal
247 to the weight of the overburden, the maximum horizontal stress (S_H) in direction of the fractures
248 (along the y-axis), and the minimum horizontal stress (S_h) perpendicular to the fractures (x-axis).
249 This background stress implies that fractures are favorably oriented for opening and propagation.
250 Figure 1 (leftmost) shows the initial geometrical setup of the domain and the fractures.

251 The background stress is defined such that
252 $$S_h = \sigma_{xx} = b_1\sigma_{zz}, \quad S_H = \sigma_{yy} = b_2\sigma_{zz}, \quad S_V = \sigma_{zz} = \rho_S g z, \qquad (4)$$
253 where ρ_S is the bulk density of the overburden, g is the acceleration of gravity, z is the depth and
254 b_1 and b_2 are positive constants. Four background stress regimes (A-D) are defined (Table 1) for
255 $b_1 = \{0.4, 0.6\}$ and for $b_2 = \{0.8, 1.2\}$. The choice of the background stress, which corresponds
256 to either a strike-slip or a normal fault regime, is based on stress settings observed in Iceland
257 (Ziegler et al., 2016), away from the central volcanism and therefore also away from the complex
258 stress conditions associated with volcanic activity.

259 Motivated by the assumption of a low rock porosity of 5%, the bulk density of the overburden is
260 set equal to that of the rock. The matrix permeability is assumed to be 10 µD and the residual
261 aperture to be 2 mm. Those values are in the lower range of what is suggested by measurements
262 in active systems (Keilegavlen et al., 2021b; Massiot et al., 2017; Sigurdsson et al., 2000). The
263 linear thermal expansion of the rock is chosen according to the temperature conditions at the two
264 different settings, with the thermal expansion coefficient for the high temperature case set five
265 times larger than for the second case, see Table 1 (Yin et al., 2021). The thermal expansion
266 coefficient of water and water viscosity is chosen according to the overall temperature, while
267 other parameters are constant, across the two different regional settings (1 and 2) shown in
268 Table 1.

269 **Table 1:** Background-stress for regimes A-B and parameters for regional settings 1&2, defining
270 conditions for the eight different cases modelled. Parameters that are identical for both settings
271 are highlighted in gray.

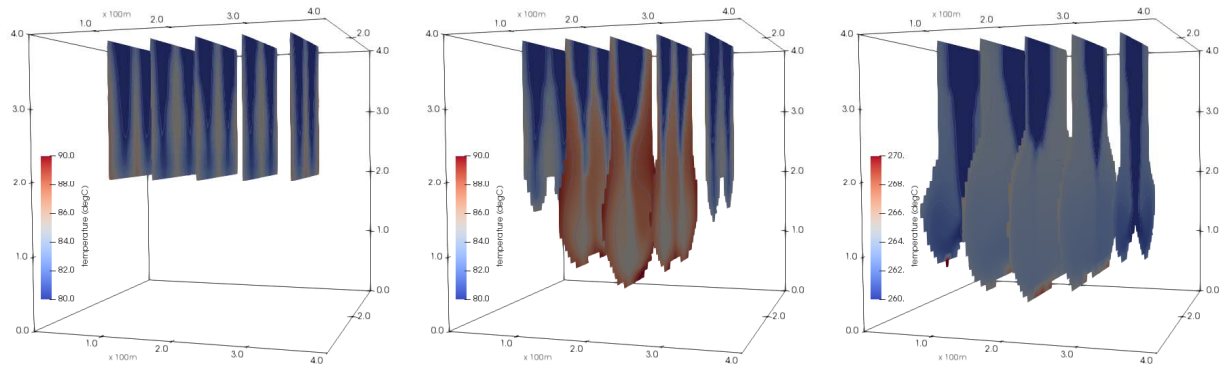| Stress regime	A	B	C	D
σ_{xx}	$0.6\,\sigma_{zz}$	$0.4\,\sigma_{zz}$	$0.4\,\sigma_{zz}$	$0.6\,\sigma_{zz}$
σ_{yy}	1.2	$1.2\,\sigma_{zz}$	$0.8\,\sigma_{zz}$	$0.8\,\sigma_{zz}$
σ_{zz}	$\rho_S g\,z$	$\rho_S g\,z$	$\rho_S g\,z$	$\rho_S g\,z$
Regional setting		1	2	
Parameter	*Symbol*	*Values*	*Values*	*Units*
Depth @top of domain	z_0	2000	1000	M
Temp. gradient with depth	dT/dz	0.13	0.08	°C/m
Temperature @top of domain	T_0	260	80	°C
Dynamic viscosity	η	1.1×10^{-4}	3.5×10^{-4}	Pa s
Fluid volumetric thermal expansion	β_f	4×10^{-4}	2×10^{-4}	°C^{-1}
Solid linear thermal expansion	β_s	5×10^{-5}	1×10^{-5}	°C^{-1}
Bulk modulus of the fluid	B_f	2.5×10^{9}	2.5×10^{9}	Pa
Bulk modulus of the rock	B_S	2.2×10^{10}	2.2×10^{10}	Pa
Biot coefficient	α	0.8	0.8	−
Reference fluid density	$\rho_{0,f}$	1×10^{3}	1×10^{3}	kg m^{-3}
Reference solid density	$\rho_{0,s}$	2.7×10^{3}	2.7×10^{3}	kg m^{-3}
Fluid specific heat	c_f	4.2×10^{3}	4.2×10^{3}	J kg^{-1} °C^{-1}
Solid specific heat	c_s	7.9×10^{2}	7.9×10^{2}	J kg^{-1} °$^{-1}$
Fluid thermal conductivity	κ_f	0.6	0.6	W m^{-1} °C^{-1}
Solid thermal conductivity	κ_s	2.0	2.0	W m^{-1} °C^{-1}
Fluid compressibility	c	4×10^{-10}	4×10^{-10}	Pa^{-1}
Shear modulus of the rock	μ	2×10^{10}	2×10^{10}	Pa
Matrix porosity	ϕ	0.05	0.05	−
Matrix permeability	k	1×10^{-17}	1×10^{-17}	m^2
Residual aperture	a_0	2.0×10^{-3}	2.0×10^{-3}	m
Friction coefficient	F	0.8	0.8	−
Dilation angle	ψ	3.0	3.0	°
Critical stress intensity factor	SI_{Icrit}	5×10^{5}	5×10^{5}	Pa

Dirichlet boundary conditions are chosen for the temperature and pressure. This means that temperature gradient and hydrostatic pressure are fixed on the sides of the numerical domain. At the top of the domain the boundary conditions are imposed on both the rock matrix and the fractures. Neumann boundary conditions are chosen for the displacement by imposing the anisotropic tractions defined in Table 1, assuming zero displacement in the centre of the bottom boundary. Considering the onset of natural convection, these boundary conditions represent a conservative choice given the prescribed linear temperature profile on the vertical boundaries.

4.2 Results

In total, eight simulations were run, representing eight different geological settings, based on the two regional settings (1-2) and the four background stress regimes (A-D). For the HT regimes, onset of propagation occurs for all the four background stress conditions shown in Table 1. For the LT regimes, onset of propagation only occurs for cases B and C.

The modelled fracture evolution can be seen in Figure 1, that shows the modeled temperature in all five fractures: Before fracture propagation (left) and at the end of the simulation (center) for setting 2C (LT, normal stress), and at the end of the simulation for setting 1A (HT, strike-slip) (right). At the end of the simulation period the middle fracture has propagated 160m and 180m downward, respectively, in the LT and HT cases. The average speed of the migrating front is therefore 3.3 and 3.5 m/year for the two different cases.
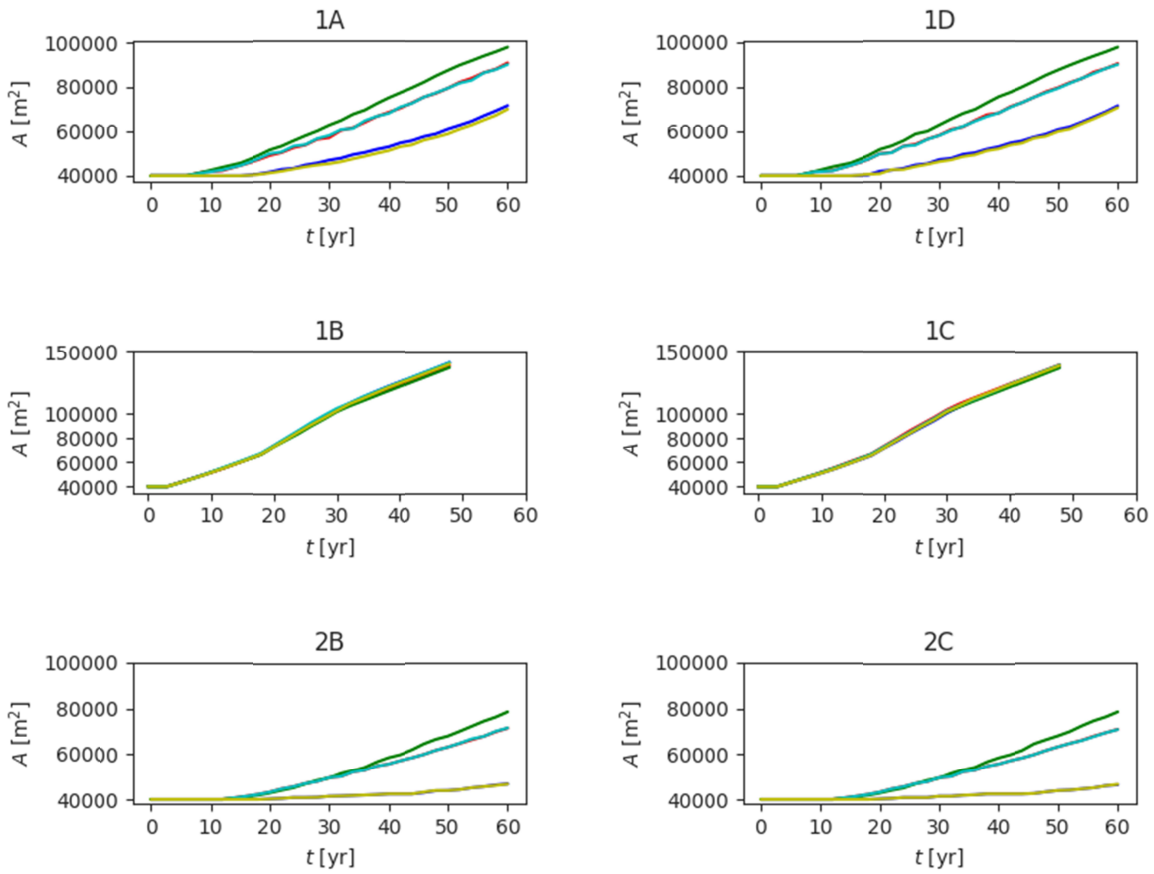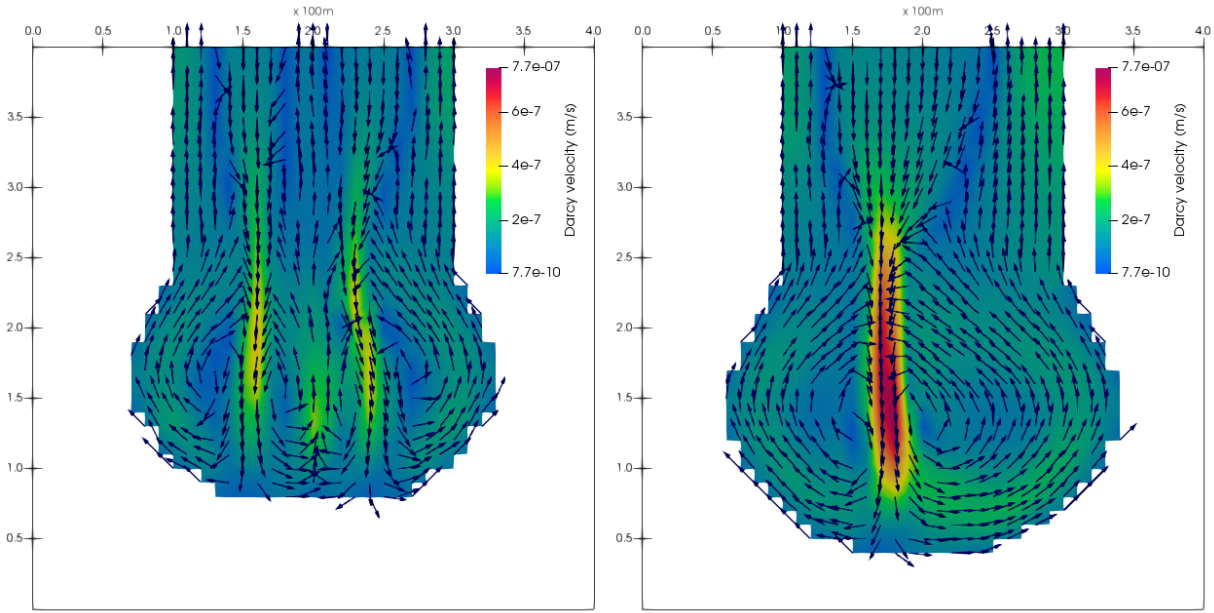
290

Figure 1: Temperature distribution in the five fractures: Left: Setting 2C (low temperature, normal stress) after 10 years simulation time (before onset of propagation), therefore, also showing the original geometry of the domain. Center: Setting 2C at the end of the simulation (60 yr.). Right: Setting 1A (high temperature, strike-slip stress) at the end of the simulation (60 yr.).

The onset of propagation and the propagation speed of the five fractures is shown in Figure 2 for the six simulations where propagation occurs. The onset of propagation in HT regimes (1A to 1D) is after 7-8 years, for the thermal expansion coefficient set according to the predicted thermal conditions at 2 km depth within the crust. However, with thermal expansion coefficient set according to the predicted thermal conditions at 1 km depth within the crust in the LT setting (2), there is no onset of propagation for stress regimes A and D, when the background minimum horizontal stress is 60% of the vertical stress. When the background minimum horizontal stress is 40% of the vertical stress (2B and 2C), the thermal stress imposed in the vicinity of the fracture is sufficient to overcome the background stress. The onset of propagation in those settings is after 12-13 years. Based on additional simulation studies, the transition to a regime of propagation is estimated to occur when the minimum horizontal stress is between 45% and 40% of the vertical stress.

In Figure 3 the Darcy velocity in the center fracture is shown for the low temperature case after 50 and 60 years. As the figure shows, fluid circulation in the fracture forms convection cells, however the flow pattern and number of cells change as the fracture propagates. This pattern is observed in both HT and LT cases and is due to changes in the fracture geometry as well as coupling to the surrounding rock matrix.

Figure 2: Propagation of the five fractures depicted as growth in surface area of each fracture. The high temperature regimes are presented in the upper two rows and the low temperature regimes in the bottom row. The left side involves a strike-slip background stress regime, and the right side a normal background stress regime.

318

Figure 3: Darcy velocity in the center fracture in setting 2C (low temperature, normal stress), with the permeability related to the aperture by the relation $K_l = a^2/12$, after 50 and 60 years simulation time (left and right, respectively).

5 Conclusions

Our results contribute to ongoing discussion on (a) the convective downward migration of fractures (CDM) in the roots of geothermal systems, and (b) CDM's importance in explaining the origin and sustainability of hydrothermal activity. Many have contributed to the development of the mathematical model and description of the phenomenon; however, the complexity of the coupled processes of fluid flow, heat transfer and fracture and rock deformation, have put limitations on its understanding. Based on numerical simulations, we show that this process is plausible in different geological settings known to host hydrothermal systems.

The results of the numerical study show that the proposed CDM is highly relevant in understanding the nature of hydrothermal systems and the origin of hydrothermal activity. Notably, the study shows that CDM is possible in settings away from central heat sources, such as magma or cooling intrusion. As proposed by Bodvarsson (1982; 1983) and Axelsson (1985), a relatively low geothermal gradient is sufficient to initiate the process. This suggestion is supported by a resent numerical study (Patterson and Driesner, 2021). We have further shown that, in the absence of a high thermal gradient (e.g., in old crust away from active zones of volcanism and spreading), the local stress settings are important. The present numerical simulations show that CDM is possible in both strike-slip and normal stress regimes. In the case of lower thermal gradient, the stress perpendicular to the fracture must be low compared to the vertical stress—as already pointed out by previous studies, but now strengthened by results of the present numerical simulation. Therefore, our results indicate that crustal stresses are a clue as to whether a hydrothermal system can evolve in regions away from volcano-tectonic activity. In the search for hidden hydrothermal activity, this could be a key factor.

Acknowledgments

347   **Open Research**

348   The data and source code for the results presented herein is available at

349   https://doi.org/10.5281/zenodo.8123952, and the results can be reproduced using version 1.4.2 of

350   PorePy (Keilegavlen et al., 2021a).

351   **References**

352   Arnórsson, S., Axelsson, G., & Sæmundsson, K. (2008). Geothermal systems in Iceland. *Jökull,*

353   *58*(1), 269–302. doi.org/10.33799/jokull2008.58.269

354

355   Axelsson G. (1985). Hydrology and thermomechanics of liquid-dominated hydrothermal systems

356   in Iceland, (Doctoral dissertation). Retrieved from ScholarsArchive@OSU.

357   (https://ir.library.oregonstate.edu/concern/graduate_thesis_or_dissertations/ms35tc96f). Oregon

358   State University.

359

360   Axelsson, G., Bjornsson, G., Egilson, T., Flovenz, O. G., Gautason, B., Hauksdottir, S., et al.

361   (2005). Nature and Properties of Recently Discovered Hidden Low-Temperature Geothermal

362   Reservoirs in Iceland. In *Proceedings of the World Geothermal Congress 2005: Antalya, Turkey,*

363   *24-29 April 2005*. Auckland, International Geothermal Association.

364

365   Axelsson, G., Flovenz, O. G., Hjartarson, A., Hauksdottir, S., Sverrisdottir, G., Arnason, F., et al.

366   (2000). Thermal energy extraction by reinjection from the Laugaland geothermal system in N-

367   Iceland. In *Proceedings of the World Geothermal Congress, 2000: Kyushu-Tohoku, Japan, May*

368   *28-June 10, 2000*. Tokyo; Auckland, Japanese Organizing Committee for WGC 2000;

369   International Geothermal Association.

370

371   Bandis, S. C., Lumsden, A. C., & Barton, N. R. (1983). Fundamentals of rock joint deformation.

372   *International Journal of Rock Mechanics and Mining Sciences & Geomechanics Abstracts,*

373   *20*(6), 249–268. doi.org/10.1016/0148-9062(83)90595-8

374

375   Barton, N. (1976). The shear strength of rock and rock joints. *International Journal of Rock*

376   *Mechanics and Mining Sciences & Geomechanics Abstracts, 13*(9), 255–279.

377   doi.org/10.1016/0148-9062(76)90003-6

378

379   Barton, N., Bandis, S., & Bakhtar, K. (1985). Strength, deformation and conductivity coupling of

380   rock joints. *International Journal of Rock Mechanics and Mining Sciences & Geomechanics*

381   *Abstracts, 22*(3), 121–140. doi.org/10.1016/0148-9062(85)93227-9

382

383   Bettison-Varga, L., Varga, R. J., & Schiffman, P. (1992). Relation between ore-forming

384   hydrothermal systems and extensional deformation in the Solea graben spreading center,

385   Troodos ophiolite, Cyprus. *Geology, 20*(11), 987–990. doi.org/10.1130/0091-

386   7613(1992)020<0987:RBOFHS>2.3.CO;2

387

388   Björnsson, G., Thordarson, S., & Steingrímsson, B. (2000). Temperature distribution and

389   conceptual reservoir model for geothermal fields in and around the city of Reykjavík, Iceland. In

390   Proceedings, Twenty-fifth Workshop on Geothermal Reservoir Engineering. (SGP-TR-165).

391   Stanford CA, Stanford University.

392

393   Björnsson, H., Björnsson, S., & Sigurgeirsson, T. (1982). Penetration of water into hot rock

394   boundaries of magma at Grímsvötn. *Nature,* 295. doi.org/10.1038/295580a0

395

396   Bjornsson, S., & Stefansson, V. (1987). Heat and Mass Transport in Geothermal Reservoirs. In J.

397   Bear & M. Y. Corapcioglu (Eds.), *Advances in Transport Phenomena in Porous Media* (pp.

398   143–183). Springer Netherlands. doi.org/10.1007/978-94-009-3625-6_5

399

400   Bodvarsson, G. (1954). Terrestrial Heat Balance in Iceland. *J. Eng. Assoc., Iceland, 39*(6), 69–

401   76.

402

403   Bodvarsson, G. (1982). Terrestrial Energy Currents and Transfer in Iceland. In G. Pálmason

404   (Ed.), *Continental and Oceanic Rifts* (pp. 271–282). American Geophysical Union (AGU).

405   doi.org/10.1029/GD008p0271

406

407   Bodvarsson, G. (1983). Temperature/flow statistics and thermomechanics of low-temperature

408   geothermal systems in Iceland. *Journal of Volcanology and Geothermal Research, 19*(3), 255–

409   280. doi.org/10.1016/0377-0273(83)90114-2

410

411 Bodvarsson, G., & Lowell, R. P. (1972). Ocean-floor heat flow and the circulation of interstitial

412 waters. *Journal of Geophysical Research (1896-1977), 77*(23), 4472–4475.

413 doi.org/10.1029/JB077i023p04472

414

415 Bozkurt, E., & Mittwede, S. K. (2005). Introduction: Evolution of continental extensional

416 tectonics of western Turkey. *Geodinamica Acta, 18*(3–4), 153–165. doi.org/10.3166/ga.18.153-

417 165

418

419 Elder, J. W. (1965). Physical Processes in Geothermal Areas. In W.H.K. Lee (Ed.), *Terrestrial*

420 *Heat Flow* (Vol. 8, pp. 211–239). American Geophysical Union (AGU).

421 doi.org/10.1029/GM008p0211

422

423 Flóvenz, Ó. G., & Saemundsson, K. (1993). Heat flow and geothermal processes in Iceland.

424 *Tectonophysics, 225*(1), 123–138. doi.org/10.1016/0040-1951(93)90253-G

425

426 Gunnarsson, G., Arnaldsson, A., & Oddsdóttir, A. L. (2000). Model Simulations of the

427 Geothermal Fields in the Hengill Area, South-Western Iceland. *Proceedings World Geothermal*

428 *Congress 2010 Bali, Indonesia, 25-29 April 2010.* International Geothermal Association

429

430 Halbach, P., Nakamura. K., Wahsner, M., Lange, J., Sakai, H., Käselitz, L., et al. (1989),

431 Probable modern analogue of Kuroko-type massive sulphide deposits in the Okinawa Trough

432 back-arc basin. *Nature,* 338, 496–499. doi.org/10.1038/338496a0

433

434   Hochstein, M. P. (2005). Heat Transfer by Hydrothermal Systems in the East African Rifts. In

435   *Proceedings of the World Geothermal Congress 2005: Antalya, Turkey, 24-29 April 2005.*

436   Auckland, International Geothermal Association.

437

438   Hochstein, M. P. (1995). Crustal heat transfer in the Taupo Volcanic Zone (New Zealand):

439   Comparison with other volcanic arcs and explanatory heat source models. *Journal of*

440   *Volcanology and Geothermal Research, 68*(1), 117–151. doi.org/10.1016/0377-0273(95)00010-

441   R

442

443   Jaffré, J., Mnejja, M., & Roberts, J. E. (2011). A discrete fracture model for two-phase flow with

444   matrix-fracture interaction. *Procedia Computer Science, 4*, 967–973.

445   doi.org/10.1016/j.procs.2011.04.102

446

447   Jolie, E., Scott, S., Faulds, J., Chambefort, I., Axelsson, G., Gutiérrez-Negrín, L. C., et al. (2021).

448   Geological controls on geothermal resources for power generation. *Nature Reviews Earth &*

449   *Environment, 2*, 324–339. doi.org/10.1038/s43017-021-00154-y

450

451   Keilegavlen, E., Berge, R., Fumagalli, A., Starnoni, M., Stefansson, I., Varela, J., & Berre, I.

452   (2021). PorePy: An open-source software for simulation of multiphysics processes in fractured

453   porous media. *Computational Geosciences, 25*(1), 243–265. doi.org/10.1007/s10596-020-10002-

454   5

455   Keilegavlen, E., Duboeuf, L., Dichiarante, A. M., Halldórsdóttir, S., Stefansson, I., Naumann,

456   M., et al. (2021). Hydro-mechanical simulation and analysis of induced seismicity for a

457   hydraulic stimulation test at the Reykjanes geothermal field, Iceland. *Geothermics,* 97, 102223.

458   doi.org/10.1016/j.geothermics.2021.102223

459

460   Kissling, W. M., & Weir, G. J. (2005). The spatial distribution of the geothermal fields in the

461   Taupo Volcanic Zone, New Zealand. *Journal of Volcanology and Geothermal Research, 145*(1),

462   136–150. doi.org/10.1016/j.jvolgeores.2005.01.006

463

464   Lapwood, E. R. (1948). Convection of a fluid in a porous medium. *Mathematical Proceedings of*

465   *the Cambridge Philosophical Society*, 44(4), 508–521. doi.org/10.1017/S030500410002452X

466

467   Limberger, J., Boxem, T., Pluymaekers, M., Bruhn, D., Manzella, A., Calcagno, P., et al. (2018).

468   Geothermal energy in deep aquifers: A global assessment of the resource base for direct heat

469   utilization. *Renewable and Sustainable Energy Reviews,* 82, 961–975.

470   doi.org/10.1016/j.rser.2017.09.084

471

472   Lister, C. R. B. (1974). On the Penetration of Water into Hot Rock. *Geophysical Journal*

473   *International, 39*(3), 465–509. doi.org/10.1111/j.1365-246X.1974.tb05468.x

474

475   Martin, V., Jaffré, J., & Roberts, J. E. (2005). Modeling Fractures and Barriers as Interfaces for

476   Flow in Porous Media. *SIAM Journal on Scientific Computing, 26*(5), 1667–1691.

477   doi.org/10.1137/S1064827503429363

478

479　Massiot, C., Townend, J., Nicol, A., & McNamara, D. D. (2017). Statistical methods of fracture

480　characterization using acoustic borehole televiewer log interpretation. *Journal of Geophysical*

481　*Research: Solid Earth, 122*(8), 6836–6852. doi.org/10.1002/2017JB014115

482

483　Murat Özler, H. (2000). Hydrogeology and geochemistry in the Curuksu (Denizli) hydrothermal

484　field, western Turkey. *Environmental Geology, 39*(10), 1169–1180.

485　doi.org/10.1007/s002540000139

486

487　Nejati, M., Paluszny, A., & Zimmerman, R. W. (2015). On the use of quarter-point tetrahedral

488　finite elements in linear elastic fracture mechanics. Engineering Fracture Mechanics, 144, 194–

489　221. doi.org/10.1016/j.engfracmech.2015.06.055

490

491　Pálmason, G. (1967). On heat flow in Iceland in relation to the Mid-Atlantic Ridge. In S.

492　Björnsson (Ed.), *Iceland and mid-ocean ridges*. Reykjavík Iceland, Vis. Isl. (Societas

493　Scientiarum Islandica).

494

495　Pálmason, G. (1981). Crustal rifting, and related thermo-mechanical processes in the lithosphere

496　beneath Iceland. *Geologische Rundschau, 70*(1), 244–260. doi.org/10.1007/BF01764325

497

498　Patterson, J. W., & Driesner, T. (2021), Elastic and Thermoelastic Effects on Thermal Water

499　Convection in Fracture Zones. *Journal of Geophysical Research: Solid Earth, 126*(2),

500　e2020JB020940. doi.org/10.1029/2020JB020940

501

502   Petersen, S., Lehrmann, B., & Murton, B. J. (2018), Modern Seafloor Hydrothermal Systems:

503   *New Perspectives on Ancient Ore-Forming Processes. Elements, 14*(5), 307–312.

504   doi.org/10.2138/gselements.14.5.307

505

506   Sigurdsson, Ó., Gudmundsson, Á., Fridleifsson, G. Ó., Franzson, H., Gudlaugsson, S. T., &

507   Stefánsson, V. (2000). Database on igneous rock properties in icelandic geothermal systems.

508   Status and unexpected results. In *Proceedings of the World Geothermal Congress, 2000:*

509   *Kyushu-Tohoku, Japan, May 28-June 10, 2000.* Tokyo; Auckland, Japanese Organizing

510   Committee for WGC 2000; International Geothermal Association.

511

512   Stefansson, I., Berre, I., & Keilegavlen, E. (2021). A fully coupled numerical model of thermo-

513   hydro-mechanical processes and fracture contact mechanics in porous media. *Computer Methods*

514   *in Applied Mechanics and Engineering, 386*, 114122. doi.org/10.1016/j.cma.2021.114122

515

516   Stefansson, I., Keilegavlen, E., Halldórsdóttir, S., & Berre, I. (2021). Numerical Modelling of

517   Convection-Driven Cooling, Deformation and Fracturing of Thermo-Poroelastic Media.

518   *Transport in Porous Media, 140*(1), 371–394. doi.org/10.1007/s11242-021-01676-1

519

520   Weir, G. (2001), Heat Output from Spreading and Rifting Models of the Taupo Volcanic Zone,

521   New Zealand. *Journal of Applied Mathematics and Decision Sciences, 5*(2), 105–118.

522   doi.org/10.1207/S15327612JAMD0502_5

523

524 White, D. E. (1968). Hydrology, activity, and heat flow of the Steamboat Springs thermal

525 system, Washoe County, Nevada. (Report No. 458C; Professional Paper). USGS Publications

526 Warehouse. doi.org/10.3133/pp458C

527

528 Xianghui, W. (2012). Reservoir assessment of the Ósabotnar low-temperature geothermal field,

529 SW-Iceland. (UNU-GTP Reports 2012 No. 38). Retrieved from GRÓ GTP

530 (https://www.grocentre.is/gtp/moya/page/msc-theses-and-fellow-projects-2012). Reykjavík,

531 UNU Geothermal Training Program.

532

533 Yang, B., Liu, J., Shi, X., Zhang, H., Wang, X., Wu, Y., & Fang, X. (2020). Mineralogy and

534 sulfur isotope characteristics of metalliferous sediments from the Tangyin hydrothermal field in

535 the southern Okinawa Trough. *Ore Geology Reviews,* 120, 103464.

536 doi.org/10.1016/j.oregeorev.2020.103464

537

538 Yin, W., Feng, Z., & Zhao, Y. (2021). Effect of Grain Size on the Mechanical Behaviour of

539 Granite Under High Temperature and Triaxial Stresses. *Rock Mechanics and Rock Engineering,*

540 *54*(2), 745–758. doi.org/10.1007/s00603-020-02303-z

541

542 Ziegler, M., Rajabi, M., Heidbach, O., Hersir, G. P., Ágústsson, K., Árnadóttir, S., & Zang, A.

543 (2016). The stress pattern of Iceland. *Tectonophysics, 674*, 101–113.

544 doi.org/10.1016/j.tecto.2016.02.008

545